Appl. Phys. B 77, 43–48 (2003)
DOI: 10.1007/s00340-003-1258-8

Applied Physics B
Lasers and Optics

M. GORKUNOV[1,✉]
B. STURMAN[2]
M. LUENNEMANN[3]
K. BUSE[3]

Feedback-controlled two-wave coupling in reflection geometry: application to lithium niobate crystals subjected to extremely high external electric fields

[1] Department of Physics, University of Osnabrück, 49069 Osnabrück, Germany
[2] International Institute for Nonlinear Studies, 630090 Novosibirsk, Russia
[3] Institute of Physics, University of Bonn, 53115 Bonn, Germany

Received: 11 June 2003
Published online: 30 July 2003 •

ABSTRACT An active stabilization of photorefractive two-wave coupling by means of an electronic feedback loop has been used extensively during recent years in transmission geometry. It leads to 100% diffraction efficiency η and also to periodic states instead of familiar steady states. We investigate the feedback operation in the case of reflection geometry, especially for iron-doped lithium niobate ($LiNbO_3$:Fe) crystals. This includes formulation of the feedback equations, numerical analysis of the operation regimes for $LiNbO_3$ crystals, and comparison between theory and experiment, which is performed in the range of applied electric fields from 0 to 650 kV cm^{-1}. The main findings are as follows: (i) the feedback does not lead to periodic states, (ii) it modifies the photorefractive response by introducing a frequency shift and maximizes η, and (iii) there is a close relation between the enhancement of η and the resonant excitation of space-charge waves predicted earlier in ferroelectric materials.

PACS 42.40.Ht; 42.65.Hw

1 Introduction

Considerable effort has been spent during recent years to understand the operation mode and potential applications of feedback-controlled photorefractive (PR) beam coupling [1–7]. Initially, it was found experimentally [1–4] that an electronic feedback loop between the output and input signal beams produces strong changes in the characteristics of two-wave coupling as well as in the diffraction properties of the recorded index grating. This feedback has allowed us to diminish the light-induced scattering, to stabilize the input light fringes, and to achieve almost 100% diffraction efficiency η of the refractive-index grating.

A first formulation of the feedback problem in terms of dynamic equations for beam amplitudes and boundary conditions was presented in [5] for the transmission (T) geometry. It adapted the idea of a $\pm\pi/2$ phase shift between the diffracted and transmitted components of the signal beam [1]. Numerical simulations of the proposed equations have shown that the system reaches quickly a state with diffraction efficiency $\eta \simeq 1$, where the ideal ($\pm\pi/2$) feedback conditions fail [5]. Thus this ideal model can be applied only to the initial stage of development.

Recently, it has been shown that inertia of the feedback loop is the key element of its permanent operation for the transmission geometry [6, 7]. As long as η is not very close to 1 or 0, this inertia is of no importance. The diffraction efficiency approaches 1 or 0 at this stage despite tilting and bending of the grating fringes caused by wave coupling. In the vicinity of these extreme values of η the phase shift between the diffracted and transmitted components of the signal beam strongly deviates from the ideal $\pm\pi/2$ values. Instead of stationary states, familiar for feedback-free wave-mixing schemes, we have periodic states: the diffraction efficiency oscillates in the close vicinity of 1 (or 0) and the input phase of the signal beam $\varphi_s(t)$ experiences strong periodic oscillations superimposed on a linear slope. This behavior is easily recognizable in experiments [6, 7].

Recently, holographic experiments in the reflection (R) geometry have become possible with $LiNbO_3$:Fe crystals owing to employment of the same feedback loop [8]. Despite extreme experimental conditions (≈ 0.1-μm grating spacing and applied electric fields up to 650 kV cm^{-1}) the data of the measurements were fully reproducible. Considerable improvements of the performance characteristics of this important PR material were achieved.

Below we investigate, both theoretically and experimentally, the impact of an active feedback loop on wave-coupling characteristics in the R-geometry. Several relevant issues have to be mentioned: (i) the results obtained earlier for the transmission geometry cannot be directly applied to the R-case. (ii) Inaccessibility of the value $\eta = 1$ in the reflection case makes one expect that the periodic states are absent and that the feedback inertia is not important. (iii) Weakly damped low-frequency eigenmodes – space-charge waves – have been predicted in the actual range of $LiNbO_3$:Fe parameters [9]. Therefore, the resonant enhancement and strong modification of the PR response can accompany the feedback operation.

2 Theoretical background

A schematic illustration of our feedback experiment is shown in Fig. 1. The signal (S) and reference (R) light beams are incident on opposite faces of the sample.

✉ Fax: +49-541/969-2351, E-mail: mgorkoun@uos.de
Permanent address: Institute of Crystallography RAS, Leninski prosp. 59, 117333 Moscow, Russia

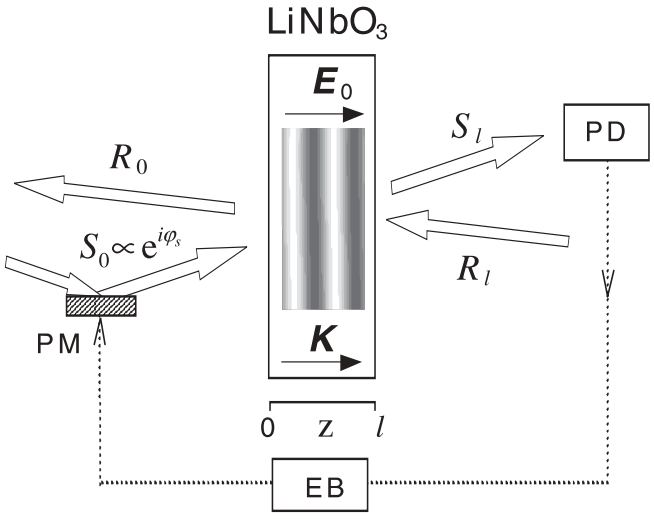

FIGURE 1 Schematic diagram of a holographic experiment in the reflection geometry with an active electronic feedback system; φ_s is the input phase governed by the feedback loop, PD is a photo-detector, EB is an electronic block, and PM is a piezo-electrically driven mirror

The propagation coordinate is z and the crystal thickness is l. The grating vector $\boldsymbol{K}$ and the applied field $\boldsymbol{E}_0$ are perpendicular to the input faces and parallel to the polar (optical) axis. The light interference and grating fringes are parallel to the input surfaces and the fringe spacing $\Lambda = 2\pi/K$ is much shorter than the light wavelength λ. The input phase of the signal beam φ_s is controlled by an electronic feedback loop via a piezo-electrically driven mirror.

The amplitudes of the signal and reference waves, S and R, obey the coupled-wave equations

$$\partial S/\partial z = +\mathrm{i}\,\kappa\, E_K\, R, \tag{1}$$

$$\partial R/\partial z = -\mathrm{i}\,\kappa\, E_K^*\, S, \tag{2}$$

where E_K is the complex amplitude of the light-induced space-charge field at the spatial frequency K, $\kappa = \pi n_o^3 r_{13}/2\lambda$, n_o is the ordinary refractive index, and r_{13} is the electro-optic constant. These equations describe Bragg diffraction from the refractive-index grating; the effect of light absorption on S and R is supposed to be negligible. The amplitude E_K is generally a function of the propagation coordinate z and time t. The intensity difference $|S(z)|^2 - |R(z)|^2$ remains constant during propagation. The amplitudes S and R are normalized in such a way that $|S_0|^2 + |R_l|^2 = 1$.

The feedback conditions for S and R can be formulated regardless of the particular form of $E_K(z,t)$; it is important only that this amplitude is changing slowly in the scale of the feedback response time. Imagine that we have blocked the input R-beam for a short time, i.e. set $R_l = 0$; see Fig. 2a. The amplitude $E_K(z,t)$ remains unchanged during this test. At the output we have the transmitted component of the signal beam S_T and the diffracted component of the reference beam R_D. Similarly, by a momentary blocking of the input S-beam (by setting $S(0,t) = 0$) we define the diffracted component of the signal beam S_D and the transmitted component of the reference beam R_T; see Fig. 2b. Since the diffractive properties of the grating can be time dependent, the introduced T- and D-amplitudes are generally functions of t. The diffraction efficiency of the grating is $\eta = |R_D|^2/|S_0|^2 \equiv |S_D|^2/|R_l|^2$; furthermore $|S_T|^2/|S_0|^2 \equiv |R_T|^2/|R_l|^2 = 1-\eta$. The reflection geometry of our problem influences strongly the values of S_D and S_T because the S- and R-beams are propagating in opposite directions.

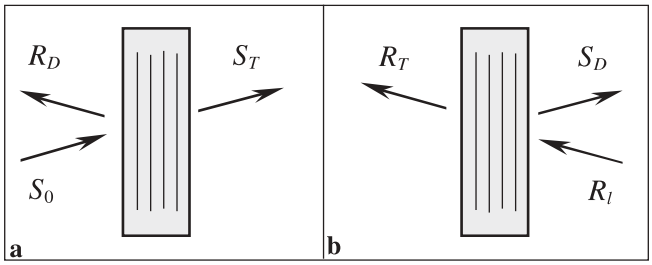

FIGURE 2 Diagram of thought experiments clarifying the meaning of the transmitted and diffracted components of the output amplitudes

As a next step we express the amplitudes S_T and S_D algebraically by the input and output amplitudes of the recording waves (see Appendix A for details). The explicit relations read

$$S_T = S_0\,\frac{|R_l|^2 - |S_l|^2}{R_0^* R_l - S_0 S_l^*}\,, \qquad S_D = R_l\,\frac{R_0^* S_l - S_0 R_l^*}{R_0^* R_l - S_0 S_l^*}\,. \tag{3}$$

They differ from the relations of the T-geometry, see [5, 7]. As long as S_D and S_T are non-zero quantities, the phase difference between them, $\Phi = \arg(S_D S_T^*)$, can be adjusted to any desirable value by a proper choice of the input phase $\varphi_s = \arg(S_0)$.

With the diffracted and transmitted components introduced, one can understand easily the experimental implementation of the feedback. Let an auxiliary (small and fast) oscillating component, $\delta\varphi_s = \psi_0 \sin(\omega t)$, be introduced into the input phase φ_s. It does not affect the recording process and serves merely for initiation of the feedback loop. The output intensity $|S(l,t)|^2 = |S_T \exp(\mathrm{i}\delta\varphi_s) + S_D|^2$ acquires high-frequency components oscillating as $\sin(\omega t)$ and $\cos(2\omega t)$. The amplitudes of these components are $I_\omega = 2|R_l S_0| \times \sqrt{\eta(1-\eta)}\,\psi_0 \sin\Phi$ and $I_{2\omega} = (1/2)|R_l S_0|\sqrt{\eta(1-\eta)}\psi_0^2 \times \cos\Phi$, where $\Phi = \arg(S_D) - \arg(S_T)$ is just the phase difference between diffracted and transmitted components of the signal beam. Using $I_{2\omega}$ as an error signal in an electronic feedback loop, one can keep $\Phi \simeq \pi/2$ (or $-\pi/2$). Thus, we have proven for the R-geometry that the feedback can be implemented regardless of dynamic distortions of the grating fringes, i.e. for $E_K(z,t) \neq const$.

The feedback equation governing the input phase φ_s is similar to that employed for the T-case [6, 7],

$$\frac{\mathrm{d}\varphi_s}{\mathrm{d}t} = \mp\frac{1}{t_f}|S_0 R_l|\sqrt{\eta(1-\eta)}\,\cos\Phi\,, \tag{4}$$

where t_f is the feedback-loop response time; it is expected to be much shorter than the PR response time. If the product $\eta(1-\eta)$ is not close to zero, the phase Φ relaxes very quickly to the value $\pi/2$ or $-\pi/2$; the feedback inertia is here of no importance. If the governing feedback signal $I_{2\omega}$ becomes very small, evolution of $\varphi_s(t)$ is controlled by this inertia.

To model the temporal evolution of the feedback-controlled two-wave coupling, we need a material equation for the grating amplitude E_K. The conventional $Fe^{2+} \leftrightarrow Fe^{3+}$

one-center charge-transport model leads to the following equation within the low-contrast approximation [9]:

$$\left(\frac{\partial}{\partial t}+\gamma_K+\mathrm{i}\omega_K\right) E_K = 2SR^*\,F_K\,. \tag{5}$$

Here $\gamma_K+\mathrm{i}\omega_K \simeq (|S|^2+|R|^2)\,(E_\mathrm{q}+E_\mathrm{D}+\mathrm{i}E_\mathrm{pv}-\mathrm{i}E_0)/E_\mathrm{q}t_\mathrm{M}$, $F_K \simeq -(E_0-E_\mathrm{pv}+\mathrm{i}E_\mathrm{D})/t_\mathrm{M}$, E_0 is the applied electric field, E_pv is the photovoltaic field [11, 12], $E_\mathrm{q} \simeq eN_\mathrm{Fe}^{2+}/\varepsilon\varepsilon_0 K$ is the saturation field, $E_\mathrm{D} = Kk_\mathrm{B}T/e$ is the diffusion field, t_M is the Maxwell relaxation time calculated for the total input intensity, e is the elementary charge, N_Fe^{2+} is the concentration of Fe^{2+} centers, ε is the static dielectric constant, ε_0 is the permittivity of free space, k_B is the Boltzmann constant, and T is the absolute temperature. All material parameters entering (5) are known (or controlled) in experiments with $LiNbO_3$:Fe. It is important that the grating spacing is very short for the R-geometry; $\Lambda \simeq 0.1\,\mu$m. This makes the saturation field E_q relatively small. By setting $N_\mathrm{Fe}^{2+} = 10^{18}\,\mathrm{cm}^{-3}$ we obtain $E_\mathrm{q} \approx 100\,\mathrm{kV\,cm}^{-1}$. The photovoltaic field E_pv does not depend on N_Fe^{2+} if the fraction of donors is relatively small; it can roughly be estimated as $\approx 100\,\mathrm{kV\,cm}^{-1}$. The diffusion field is considerably smaller, $E_\mathrm{D} \simeq 16\,\mathrm{kV\,cm}^{-1}$. The applied field E_0 can be considerably larger than E_q, E_pv, and E_D in our experiments.

The main outcome of (5) and the above estimates is as follows: suppose that $|E_0-E_\mathrm{pv}| \gg E_\mathrm{q}$, E_D; then $|\omega_K| \gg \gamma_K$, i.e. there is a weakly damped space-charge wave with the eigenfrequency ω_K. With a zero frequency shift between S- and R-beams we have $E_K \approx \mathrm{i}mE_\mathrm{q}$ in steady state; this corresponds to $\approx \pi/2$ phase shift between the light and index fringes and to power transfer into one of the recording beams. Let now the frequency shift between S- and R-beams, Ω, be equal to the eigenfrequency ω_K, which corresponds to the resonant excitation of the eigenmode. Then we have in steady state:

$$E_K \simeq (\omega_K/\gamma_K)\,mE_\mathrm{q}\,. \tag{6}$$

The grating has become non-shifted (the power transfer suppressed) and its amplitude is enhanced by a factor of $|\omega_K|/\gamma_K \gg 1$.

Relation (6) possesses a remarkable feature. Being applied to the case $m \approx 1$, it leads to the fundamental grating amplitude E_K larger than the saturation field E_q. In reality, the low-contrast approximation fails here and the function $E_K(m)$ saturates on the level of $\approx E_\mathrm{q}$. A similar situation is known for the resonant enhancement in fast PR materials [10]. To take into consideration the saturation effect, we have replaced in (5) the damping constant γ_K by $\gamma_K/(1-|E_K/cE_\mathrm{q}|^2)$, where $c \approx 1$ is a fitting parameter. Being fairly simple, this phenomenological method allows us to keep the major features of the resonant PR response [9].

Experience shows that the feedback tends to maximize the diffraction efficiency of the grating in the transmission geometry. If this assertion is applicable to the reflection case, then one can expect that the feedback will bring the system automatically to the resonant excitation of a non-shifted index grating.

Lastly, we comment on the difference between the R- and T-geometries with regard to feedback operation. In the T-case, the diffraction efficiency of the index grating, η, can reach a unit value for finite grating amplitude and thickness. Just this feature is responsible for strong periodic oscillations of the input phase φ_s in addition to its linear growth or decrease [6, 7]. In the R-case, the diffraction efficiency can never reach unity. Hence, no periodic states are expected here.

3 Numerical simulations

In our theoretical studies of the feedback-controlled two-wave coupling we have solved numerically (1), (2), and (5) together with the feedback equation (4). The feedback-loop response time t_f ranged from 10^{-3} to 10^{-4} of the Maxwell time t_M. It was found that the signs + and − in this equation ensure stabilization for $E_0-E_\mathrm{pv}<0$ and $E_0-E_\mathrm{pv}>0$, respectively.

Consider first the case of unit input beam ratio, $\beta = |S_0|^2/|R_l|^2 = 1$. The system arrives here quickly (for $t=(2-3)t_\mathrm{M}$) at steady state where there is no noticeable energy exchange between the S- and R-beams, i.e. $m(z)=1$. The input phase of the signal wave φ_s grows linearly in time, which means introduction of a constant frequency shift Ω between the recording beams.

Figure 3a shows the dependence $\Omega(E_0)$ calculated for $E_\mathrm{pv} = 100\,\mathrm{kV\,cm}^{-1}$ and $N^{2+} = 0.7\times10^{18}\,\mathrm{cm}^{-3}$. For $E_0 \gtrsim$

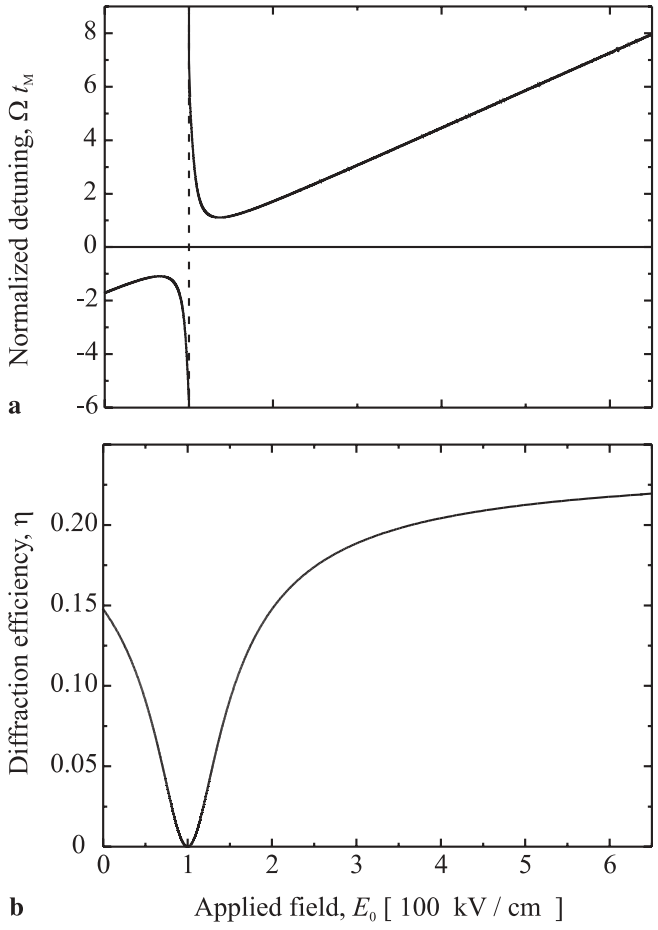

FIGURE 3 Field dependence of frequency shift Ω (**a**) and diffraction efficiency η (**b**) for the feedback-controlled steady state with $\beta=1$, $N^{2+}=0.7\times10^{18}\,\mathrm{cm}^{-3}$, and $l=0.22\,\mathrm{mm}$

E_{pv} this dependence is practically linear and very close to the field dependence of the eigenfrequency $\omega_K(E_0)$. Thus, the expected linear excitation of space-charge waves takes place. The phase difference Φ is very close to $\pi/2$ when the applied field E_0 exceeds the photovoltaic field E_{pv}; the feedback inertia is not important in this region. With E_0 approaching E_{pv} from above, the frequency detuning Ω grows steeply, tending to infinity. The phase Φ deflects here strongly from $\pi/2$ and the feedback inertia is very important; the smaller t_f, the stronger is the growth of Ω. This means that there is no steady state that meets the ideal feedback conditions at $\beta = 1$ for the diffusion PR response.

The field dependence of the steady-state diffraction efficiency $\eta(E_0)$ is shown in Fig. 3b. It possesses a clearly pronounced minimum at $E_0 \approx E_{pv}$ (where η is very small) and shows a saturation for $E_0 \gg E_{pv}$. The saturated value of $\eta(E_0)$ is not close to unity so that the feedback signal $I_{2\omega}$ is far from zero. The minimum value of η is controlled by the feedback response time; the longer t_f, the larger is η_{min}. The origin of such low values of η for $E_0 \approx E_{pv}$ is evidently the large frequency detuning causing a running interference pattern and hence strong erasure. The charge saturation is negligible in this region since $|E_K| \ll E_q$. Note lastly that the feedback maximizes η only for $|E_0 - E_{pv}| \gtrsim E_D$.

Now we turn to the case of small contrast, $m \ll 1$. Two opposite tendencies affect here the beam coupling in the region of large fields. On the one hand, the feedback tends to exploit the resonance $\Omega = \omega_K$ to maximize E_K and η; the contrast m remains small within this scenario because of no power transfer to the weakest beam. On the other hand, the feedback can try to keep $\Omega \approx 0$ to initiate the power transfer into the weakest beam; this allows us to increase the contrast and can also be advantageous for increasing η.

Lastly we present numerical data for the steady state. Figure 4 shows the spatial profiles of the beam intensities, the light contrast, the grating amplitude, and the phase shift between the index and light fringes. One can see that the spatial distributions combine the features of the two expected scenarios. In the right-hand part of the sample the recorded grating is almost $\pi/2$ shifted; this leads to decreasing intensity ratio $|S(z)|^2/|R(z)|^2$ and increasing contrast $m(z)$ and amplitude $|E_K(z)|$ when the coordinate z is changing from l to $l/2$. In the left-hand part of the sample the grating becomes almost non-shifted; the energy transfer is weak here and the contrast $m(z) \simeq 0.6$ is much higher than its input value. This is the region of resonant enhancement. Since the total energy $|S(z)|^2 + |R(z)|^2$ is changing across the crystal, the resonant condition $\Omega = \omega_K$ cannot be fulfilled simultaneously in the whole crystal; in our case Ω is much larger than ω_K in the right-hand half of the sample. The calculated function $\Omega(E_0)$ is strictly linear for $E_0 \gtrsim 1.5E_{pv}$; it exceeds $\omega_K(E_0)$ calculated for the input intensity $|S_0|^2 + |R_l|^2$ by a factor of ≈ 1.2.

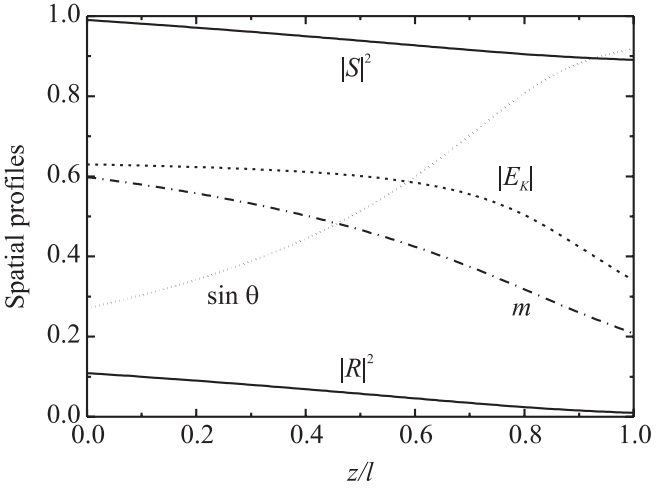

FIGURE 4 Spatial characteristics of the feedback-controlled two-wave coupling for $\beta = 100$, $N^{2+} = 0.7 \times 10^{18}\,\mathrm{cm}^{-3}$, $l = 0.22\,\mathrm{mm}$, and $E_0 = 600\,\mathrm{kV\,cm}^{-1}$. The intensities of signal and reference waves are $|S|^2$ and $|R|^2$, $|E_K|$ is the absolute value of the amplitude of the space-charge field (measured in $10^5\,\mathrm{V\,cm}^{-1}$), m is the modulation degree (the input contrast $m_0 \simeq 0.2$), and $\sin\theta$ is the sine of the phase shift θ between the index and light patterns

4 Experiment

In our experiments we use a congruently melting iron-doped $LiNbO_3$ crystal with an iron concentration of $N_{Fe} \simeq 18 \times 10^{18}\,\mathrm{cm}^{-3}$ and a thickness $l = 0.22\,\mathrm{mm}$. The polar (optical) axis is perpendicular to the input faces. The absorption coefficient α ranges from 3.0 to $9.9\,\mathrm{cm}^{-1}$ at 477 nm when the donor concentration N^{2+} ranges from ≈ 0.7 to $\approx 2.3 \times 10^{18}\,\mathrm{cm}^{-3}$. The fraction of Fe^{2+} ions was varied by annealing treatments [13, 14].

The sample is placed in a Plexiglas holder and the input surfaces are contacted with transparent liquid electrodes, see [8] for more detail. The applied electric field ranges from 0 to $650\,\mathrm{kV\,cm}^{-1}$ and is parallel to the polar axis. Application of larger fields leads to electric breakdown. Equally strong fields of the opposite direction would invert the spontaneous polarization.

Two-wave-coupling experiments are carried out in the R-geometry using a standard interference setup supplemented by a stabilization feedback loop [2, 3]. Two pump beams from an argon-ion laser ($\lambda = 488\,\mathrm{nm}$) are incident on opposite faces of the sample at small angles with regard to the surface normal; the corresponding grating spacing Λ is approximately 105 nm. The total input intensity is $\approx 0.18\,\mathrm{W\,cm}^{-2}$. The temporal evolution of the output intensities $|R_0|^2$ and $|S_l|^2$, the diffraction efficiency of the recorded index grating, as well as the feedback signal driving the input phase of the signal beam, φ_s, are measured.

We have mentioned first that the feedback sign (the sign of the error signal $I_{2\omega}$) has to be different in the regions $E_0 - E_{pv} < 0$ and $E_0 - E_{pv} > 0$ to ensure maximization of diffraction efficiency. This observation is in full agreement with the theoretical predictions.

By monitoring the piezo-signal driving the input phase φ_s we have found that it is generally linear in steady state; no periodic (or quasi-periodic) oscillations of this signal were found. The time derivative of the input phase $\Omega = \mathrm{d}\varphi_s/\mathrm{d}t$ was negative for $E_0 \lesssim 100\,\mathrm{kV\,cm}^{-1}$ and positive for $E_0 \gtrsim 200\,\mathrm{kV\,cm}^{-1}$. Our experimental data on the field dependence of the detuning Ω are presented in Fig. 5. One sees that the experimental dots are well fitted by a linear function. Furthermore, we have estimated that the maximum value of Ω exceeds the reciprocal Maxwell time t_M^{-1}

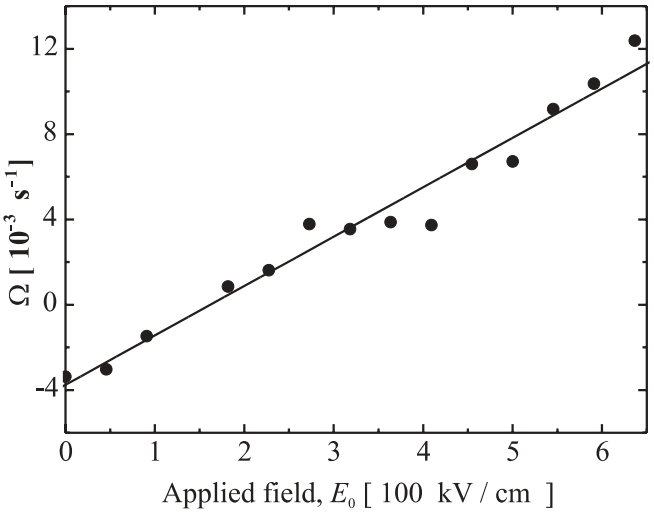

FIGURE 5 Frequency detuning Ω versus applied field E_0 for $\beta = 1$ and $N^{2+} = 0.7 \times 10^{18}$ cm^{-3}. The *filled dots* are experimental data and the *solid line* is a linear fit

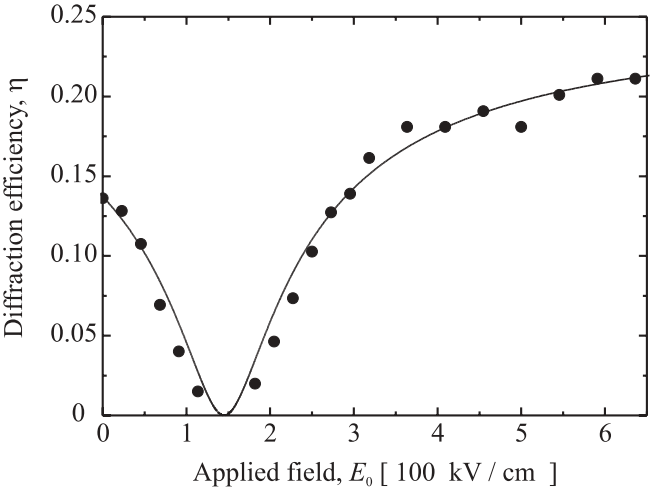

FIGURE 6 Diffraction efficiency η versus applied field E_0 for $\beta = 1$ and a donor concentration $N^{2+} \simeq 1.1 \times 10^{18}$ cm^{-3} ($\alpha \simeq 5$ cm^{-1}). The *filled squares* are experimental data and the *solid curve* is the result of numerical simulation for $c = 2/3$

by a factor of ≈ 4.3 in our experiment. This is not far from the data of Fig. 3. The main source of a spread of experimental dots are fluctuations of the input phase difference which are compensated by the feedback loop. Extreme precautions are necessary to diminish these fluctuations strongly.

Within the range $100\,\mathrm{kV\,cm^{-1}} \lesssim E_0 \lesssim 200\,\mathrm{kV\,cm^{-1}}$ operation of the feedback loop was not stable enough to ensure reproducible measurements of the frequency shift. Only some qualitative indications of increasing $|\Omega(E_0)|$ for E_0 approaching E_{pv} were found.

Lastly, we present the results on the field dependence of the diffraction efficiency η. The experimental data for $\beta = 1$ and the theoretical fit are shown in Fig. 6. The agreement between experiment and theory is pretty good. Note that the use of the fitting parameter c, which controls the saturation level of the amplitude E_K, is a crucial element of our simulations of the feedback operation.

5 Summary

The main results of this paper can be summarized as follows:

- It is shown theoretically for the reflection geometry that the $\pm\pi/2$ feedback conditions for stabilization of two-wave coupling can be implemented regardless of dynamic distortions of the grating fringes.
- It is shown theoretically and experimentally that the feedback loop does not lead to periodic states in the reflection geometry, in contrast to the transmission configurations.
- It is proven theoretically and experimentally that the feedback operation is not reduced to stabilization of the light fringes; it introduces generally a frequency detuning between the incident light beams, i.e. a moving space-charge grating arises.
- It is shown theoretically for $LiNbO_3$:Fe crystals that the feedback-introduced detuning Ω is resonant to the eigenfrequency ω_K of the space-charge waves predicted earlier for the R-geometry and large driving field $E_0 - E_{\mathrm{pv}}$.
- It is proven experimentally that the feedback-introduced frequency detuning Ω is proportional to $E_0 - E_{\mathrm{pv}}$ in the region of large applied field and can be identified with the eigenfrequency ω_K. Thus, a resonant excitation of space-charge waves and strong modification of the photorefractive response take place.

Appendix A: calculation of S_{T} and S_{D}

Equations (1) and (2) describe a variety of diffraction (readout) processes for the recorded grating of the amplitude $E_K = E_K(z)$. These processes are distinguished by the input values of the light amplitudes. Each particular readout process can be described in a simple algebraic manner if we know the recording amplitudes $S(z)$ and $R(z)$. To prove it, we point out that the general solution $\bar{S}$ and $\bar{R}$ of the linear set of differential equations (1) and (2) with a 'frozen' grating profile $E_K(z)$ can be presented as

$$\begin{pmatrix} \bar{S} \\ \bar{R} \end{pmatrix} = c_1 \begin{pmatrix} S_1 \\ R_1 \end{pmatrix} + c_2 \begin{pmatrix} S_2 \\ R_2 \end{pmatrix} , \tag{A.1}$$

where $S_1(z)$, $R_1(z)$ and $S_2(z)$, $R_2(z)$ are two independent particular solutions of the set (1) and (2) and $c_{1,2}$ arbitrary constants. As the first solution we use the recording amplitudes, $S_1 = S$ and $R_1 = R$. By taking the complex conjugate of (1) and (2), one can make sure that $S_2 = R^*$ and $R_2 = S^*$ can be chosen as the second independent solution.

To find the transmitted amplitude S_{T}, we have to consider the particular solution $\bar{S}$ and $\bar{R}$ meeting the boundary conditions $\bar{S}(0) = S_0$ and $\bar{R}(l) = 0$. From here and (A.1) one can easily express $c_{1,2}$ through the boundary values of the recording amplitudes S_0, S_l, R_0, and R_l. By calculating $S_{\mathrm{D}} = \bar{S}(l)$ from (A1) we arrive at the necessary explicit expression, see (3). The diffracted component $S_{\mathrm{D}} = \bar{S}(l)$ can be calculated similarly; it corresponds to the boundary conditions $\bar{S}(0) = 0$ and $\bar{R}(l) = R_l$.

ACKNOWLEDGEMENTS Financial support from the Deutsche Forschungsgemeinschaft and from the Deutsche Telekom AG is gratefully acknowledged.

REFERENCES

1 A. Freschi, J. Frejlich: J. Opt. Soc. Am. B **11**, 1837 (1994)
2 P.M. Garcia, K. Buse, D. Kip, J. Frejlich: Opt. Commun. **117**, 35 (1995)
3 P.M. Garcia, A.A. Freschi, J. Frejlich, E. Krätzig: Appl. Phys. B **63**, 207 (1996)
4 A. Freschi, P.M. Garcia, J. Frejlich: Opt. Commun. **143**, 257 (1997)
5 V.P. Kamenov, K.H. Ringhofer, B.I. Sturman, J. Frejlich: Phys. Rev. A **56**, R2541 (1997)
6 E.V. Podivilov, B.I. Sturman, S.G. Odoulov, S.L. Pavlyuk, K.V. Shcherbin, V.Y. Gayvoronsky, K.H. Ringhofer, V.P. Kamenov: Opt. Commun. **192**, 399 (2001)
7 E.V. Podivilov, B.I. Sturman, S.G. Odoulov, S.L. Pavlyuk, K.V. Shcherbin, V.Y. Gayvoronsky, K.H. Ringhofer, V.P. Kamenov: Phys. Rev. A **63**, 053805-1 (2001)
8 M. Luennemann, U. Hartwig, K. Buse: J. Opt. Soc. Am. B **20**, N8 (2003)
9 B.I. Sturman, E. Shamonina, M. Mann, K.H. Ringhofer: J. Opt. Soc. Am. B **9**, 1642 (1995)
10 L. Solymar, D.J. Webb, A. Grunnet-Jepsen: *The Physics and Applications of Photorefractive Materials* (Clarendon, Oxford 1996)
11 A.M. Glass, D. von der Linde, T.J. Negran: Appl. Phys. Lett. **25**, 233 (1974)
12 B.I. Sturman, V.M. Fridkin: *The Photovoltaic and Photorefractive Effects in Noncentrosymmetric Materials* (Gordon and Breach, Philadelphia 1992)
13 J.J. Amodei, W. Phillips, D.L. Staebler: Appl. Opt. **11**, 390 (1972)
14 G.E. Peterson, A.M. Glass, T.J. Negran: Appl. Phys. Lett. **19**, 130 (1971)